MATHEMATICAL MODELING AND COMPUTING, Vol. 9, No. 1, pp. 83–91 (2022)

Modeling Computing Mathematical

Effect of suction and MHD induced Navier slip flow due to a non-linear stretching/shrinking sheet

Alias N. S.[1], Hafidzuddin M. E. H.[2]

[1] *Department of Mathematics, Universiti Putra Malaysia, 43400 UPM Serdang, Selangor, Malaysia*
[2] *Centre of Foundation Studies for Agricultural Science, Universiti Putra Malaysia, 43400 UPM Serdang, Selangor, Malaysia*

(Received 7 July 2021; Accepted 16 November 2021)

In this study, a problem of a magnetohydrodynamic (MHD) induced Navier slip flow over a non-linear stretching and shrinking sheet with the existence of suction is considered. Similarity transformation is used to transform the governing nonlinear partial differential equations into a system of nonlinear ordinary equations. The transformed ordinary differential equations are then solved by using the Shooting Method in Maple software. Dual solutions are obtained for certain governing parameters. The results obtained show that suction improves skin friction, while the slip parameter reduces shear wall stress. Moreover, it is established that the range of dual solutions for stretching sheet is smaller compared to the shrinking case.

Keywords: *MHD, Navier slip, stretching/shrinking sheet, non-linear, dual solution.*
2010 MSC: 76W05 **DOI:** 10.23939/mmc2022.01.083

1. Introduction

It is reported that the work on the dynamics of the boundary layer flow over a stretching surface was pioneered by Crane [1], for which he found the exact solution of the two-dimensional Navier–Stokes equations. Since then, there have been many researches done over a stretching surface over numerous conditions, to cite a few [2–11]. Meanwhile, the flow of an incompressible fluid due to a shrinking sheet acquires attention for its abnormal behaviour in the flow dynamics because very little is known about said sheet, where the velocity on the boundary is moving towards a fixed point. A very specific unsteady shrinking film solution was discussed by Wang [12]. Miklavcic and Wang [13] studied the properties of a viscous flow due to a shrinking sheet with suction and found out that the flow is unlikely to exist unless adequate suction on the boundary is imposed, since vorticity of the shrinking sheet is not confined within a boundary layer. To maintain boundary layer structure, the flow needs a certain amount of external suction at the porous sheet. Fang and Zhang [14] obtained a closed formed analytical solution for steady MHD flow over a porous shrinking subject to applied suction. Next, Fang et al. [15] found out the exact analytic solution of the thermal boundary layer over a shrinking sheet with a mass transfer. Moreover, the solution obtained is also an exact solution of the governing Navier–Stokes equations for that problem, and they reported greatly different solution behavior with multiple solution branches compared to the corresponding stretching sheet problem. After awhile, Fang et al. [16] gained the exact solution for the viscous flow over a shrinking sheet with a second order slip flow model by solving analytically.

In fluid dynamics, magnetohydrodynamics (MHD) is a condition where there is an electrically conducting fluid in the presence of electric and magnetic field. The earliest researcher to consider the magnetohydrodynamic flow on non-Newtonian fluid whose magnetic field is perpendicular to the direction of the flow was Sarpkaya [17]. Then, Pavlov [18] improvised the research by studying the

This work was supported by grant GP-UPM/2018/9619000 from University Putra Malaysa, Malaysia.

MHD boundary layer flow of an electrically conducting fluid due to the stretching of a plane elastic surface in the presence of a uniform transverse magnetic field and achieved an exact similarity solution of this problem. Mahabaleshwar et al. [19] examined the MHD flow of an electrically conducting Newtonian fluid over a super linear stretching sheet in the presence of suction/injection and Navier slip by using modified Adomain decomposition method (MADM) and Pade approximants, and they found that Navier's slip condition can lead to a non-essential growth of the boundary layer thickness and a decrease in the axial and transverse velocities. Recently, Abdal et al. [20] investigated the multislip effects on the magnetohydrodynamic (MHD) mixed convection unsteady flow of micropolar nano-fluids over a stretching/shrinking sheet along with radiation in the presence of a heat source.

Most of the studies support the validity of the Dirichlet–Stokes no-slip condition, that is, the velocity vanishes on the boundaries. However, it's all started when Navier [21] presented a slip-with-friction boundary condition and stated that the component of the fluid velocity tangent to the surface should be proportional to the rate of strain at the surface. The velocity of component normal to the surface is zero because mass cannot penetrate an impermeable solid surface. Recent experiments, generally with typical dimensions of microns or smaller, have demonstrated that the phenomenon of slip actually occurs.

Over the last few years, various investigations have also been made to study various flow problems of Newtonian and non-Newtonian fluids with or without the Navier slip boundary condition. For example, some Navier conditions for the close Stokes–Fourier system from Maxwell conditions (combining perfect/specular reflection and diffuse/Gaussian reflection) for the Boltzmann equations is derived by Masmoudi and Saint–Raymond [22]. Iftimie and Sueur [23] investigated inviscid limit of the incompressible Navier–Stokes equations when the Navier slip-with-friction conditions are prescribed on impermeable boundaries and developed a descriptive method which able to precisely describe the error, both in two dimensions and three dimensions. Then, Das and Jana [24] investigated the combination effects of magnetic field, suction/injection and Navier slip on the entropy generation in an MHD flow through a porous channel and Matin and Khan [25] proposed the effect of boundary slip on the purely pressure driven flow of a viscoelastic biofluid through a nanofluidic channel. Then, Tlili et al. [26] focus on the effects of magnetic field, Navier slip and convective heat of nanofluid flow over a wedge.

Motivated by the above-mentioned studies, this research extends the work done Mahabaleshwar et al. [19] by including both the shrinking and suction parameters. The governing partial differential equations are first transformed into a system of ordinary differential equations, and then solved numerically by using the built-in Shooting method in MAPLE.

2. Problem Formulation

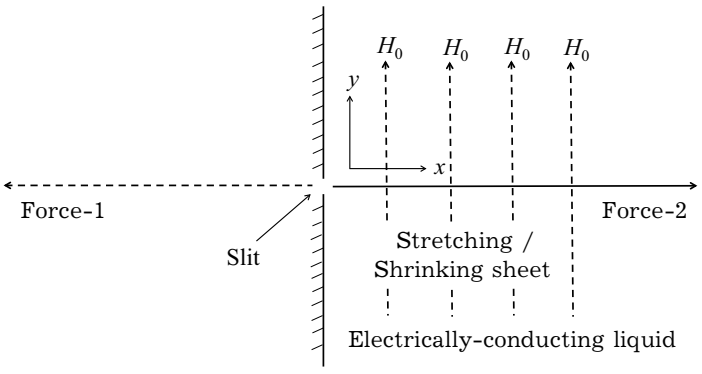

Fig. 1. Schematic of the stretching/shrinking problem.

Consider a steady-state laminar non-compressible viscous fluid flow over a non linear stretching or shrinking sheet with the existence of magnetic field, Navier slip condition and suction using boundary layer approximation, where the lateral surface velocity is proportional to the distance x from the origin. The sheet is stretched/shrunk in a nonlinear way along the x-axis and y-direction is taken for fluid flow with the origin fixed, as shown in Fig. 1. It is assumed that the sheet is stretched/shrunk with the velocity $\lambda u(x)$, where λ is for stretching ($\lambda > 0$) or shrinking ($\lambda < 0$) parameter, a non-uniform transverse magnetic field of strength H_0 is applied normal to the sheet, and the induced magnetic field is neglected due to small magnetic Reynolds number, Re.

Under these assumptions, the fundamental laminar boundary layer equations for the stretching and shrinking flow can be written as

$$\frac{\partial u}{\partial x}+\frac{\partial v}{\partial y}=0, \tag{1}$$

$$u\frac{\partial u}{\partial x}+v\frac{\partial v}{\partial y}=\nu\frac{\partial^2 u}{\partial y^2}-\frac{\sigma H^2(x)}{\rho}u. \tag{2}$$

We take $R_m \ll 1$, where R_m is the magnetic Reynolds number and ν is the fluid kinematic viscosity which is constant for this case, fluid density ρ and electrical conductivity σ, and therefore defining the magnetic field as

$$H(x)=H_0\,x^{\frac{n-1}{2}}. \tag{3}$$

Here, we define the sheet as permeable and lateral mass transfer with a certain velocity distribution $v_w(x)$ is given. The boundary conditions corresponding to the non linear stretching and shrinking sheet are given below

$$\begin{aligned} &u(x,0)-\lambda\,c\,x^n=k\,\nu\frac{\partial u}{\partial y}(x,0), \quad v_w(x,0)=v_w(x),\\ &u(x,\infty)=0. \end{aligned} \tag{4}$$

We take (x,y) as the respective normal directions with corresponding velocities (u,v). A continuous surface with non linear stretching and shrinking speed is pressed into a laminar boundary layer flows along the x direction are $u(x,0)=\lambda\,c\,x^n$, where the stretching and shrinking rate λc is constant ($\lambda>0$ for stretching sheet and vise versa) and n is the nonlinear constant, $v_w(x)$ is the mass velocity with $v_w(x)<0$ for suction, $v_w(x)>0$ for injection and $v_w(x)=0$ is the case when the surface is impermeable.

The conservation of mass satisfied the physical stream function $\psi(x,y)$ and can be expressed as

$$u=\frac{\partial\psi}{\partial y}, \quad v=-\frac{\partial\psi}{\partial x}. \tag{5}$$

Next, $\eta=\sqrt{\frac{c(n+1)}{2\nu}}x^{\frac{n-1}{2}}y$ is defined as asimilarity variable and consequently the axial and transverse velocities can be written as

$$u=c\,x^n f'(\eta), \quad v=-\sqrt{\frac{c\,\nu(n+1)}{2}}x^{\frac{n-1}{2}}f(\eta)+\left[\frac{n-1}{n+1}\right]\eta\,f'(\eta). \tag{6}$$

Using the above transformations, Eq. (1) is satisfied, while Eq. (2) can be expressed as

$$f'''+ff''-\beta f^2-Qf'=0, \tag{7}$$

while the boundary conditions (4) are reduced to

$$\begin{aligned} &f(0)=s, \quad f'(0)=\lambda+\Gamma f''(0),\\ &f'(\eta)=0 \quad \text{as} \quad \eta\to\infty. \end{aligned} \tag{8}$$

where $s=-\frac{v_w(x)}{\sqrt{\frac{c(n+1)}{2\nu}}x^{\frac{n-1}{2}}}$ represents suction ($s>0$) or injection ($s<0$) parameter, $\lambda>0$ is for the stretching sheet and $\lambda<0$ is for the shrinking sheet, and $\Gamma=k\,\nu\sqrt{\frac{c(n+1)}{2\nu}}x^{\frac{n-1}{2}}$ is the Navier's slip parameter.

The physical quantity of practical interest is the skin friction coefficient C_f, which is given by

$$C_f = \frac{\tau_w}{\rho\, u^2}, \tag{9}$$

where τ_w is a shear stress in x-direction and is noted by

$$\tau_w = \mu \left(\frac{\partial u}{\partial y}\right) \tag{10}$$

with μ refers to the fluid dynamic viscosity for the fluid. Using (6), (9) and (10), we have

$$\sqrt{\frac{(n+1)}{2}}(\mathrm{Re})^{1/2} C_f = f''(0), \tag{11}$$

where $\mathrm{Re} = \frac{\nu}{u\,x}$ is a Reynold's number.

3. Results and Discussion

The problem of nonlinear ordinary differential equation (7) along with the boundary condition (8) have been figured out numerically using the Shooting Method via Maple software. Initially, the accuracy of this method has been validated by comparing the present results with the values obtained from previous literature. Table 1 represents the excellent comparison for the values of $f''(0)$ with the increasing of Chandrasekhar number, Q. This comparison proved that the method used in this problem is accurate and precise.

Table 1. Comparison of $f''(0)$ for $s = 0$, $\lambda = 1$, $\beta = 1$, $\Gamma = 0$.

Q	Present results	[19]
0	−1.00066	−1.00018
1	−1.41421	−1.41421
5	−2.44948	−2.44943
10	−3.31662	−3.31656

The effects of stretching or shrinking parameter λ, suction parameter s, slip parameter Γ and the nonlinear parameter β towards the skin friction coefficient $f''(0)$ and velocity profiles $f'(\eta)$ are represented in graphs. In addition, the variations of skin friction coefficient $f''(0)$ with stretching/shrinking λ and suction parameter s are also illustrated. The addition of suction and shrinking sheet to the previous problem considered by [19] is seen to produce more than one solution.

Table 2. Values of λ_c for different values of s when $\Gamma = 0.5$, $Q = 0.1$, $\beta = 1$.

s	$(\lambda_c,\ f''(0))$
2.3	(−2.3155, 1.8803)
2.5	(−2.8007, 2.3815)
2.7	(−3.3401, 2.9108)

Table 3. Values of s_c for different values of λ when $\Gamma = 0.5$, $Q = 0.1$, $\beta = 1$.

λ	$(s_c,\ f''(0))$
−0.5	(1.0755, 0.2216)
−0.75	(1.3499, 0.3900)
−1	(1.6111, 0.5211)

Table 4. Values of λ_c for different values of Γ when $s = 2.5$, $Q = 0.1$, $\beta = 1$.

Γ	$(\lambda_c,\ f''(0))$
0.1	(−1.8764, 2.1986)
0.5	(−2.8007, 2.3815)
0.75	(−3.4018, 2.4175)

Fig. 2 illustrates the skin friction coefficient $f''(0)$ with stretching/shrinking parameter λ for some values of suction s when $\Gamma = 0.5$, $Q = 0.1$ and $\beta = 1$, while Fig. 3 represents $f''(0)$ with s for some values of λ when $\Gamma = 0.5$, $Q = 0.1$, $\beta = 1$. Moreover, the variations of $f''(0)$ with λ for different values of slip Γ when $s = 2.5$, $Q = 0.1$, $\beta = 1$ are shown in Fig. 4. Based on these illustrations, it is obviously shown that there are two visible solutions for both shrinking ($\lambda < 0$) and stretching ($\lambda > 0$) cases whereas the solid lines represent the first solution and the dotted lines represent the second solution. The critical values of λ and s are represented by λ_c and s_c, respectively. It indicates the existence of multiple solutions for $\lambda_c < \lambda$ and $s_c < s$ while unique solution when $\lambda = \lambda_c$ and $s = s_c$. The boundary layer separates from the surface in the no solution area, therefore, there is no more solution since the boundary layer approximation method is no longer used.

Fig. 2 demonstrates the effect of suction parameter s for $s > 0$ on skin friction coefficients $f''(0)$. The values of $f''(0)$ for the first solution are moderately increasing with the step up of suction values and contrarily for second solution. The wall shear stress increases as s increases for the first solution while it works oppositely for the second solution. In addition, it is observed that the values of $|\lambda_c|$ increase when s increases. The shrinking case gives larger values for $f''(0)$ compared with the stretching sheet case. Opposite flow of fluid caused by the slow motion of flow along the shrinking sheet which consequently effect the separation of boundary layer and therefore raising the skin friction coefficient.

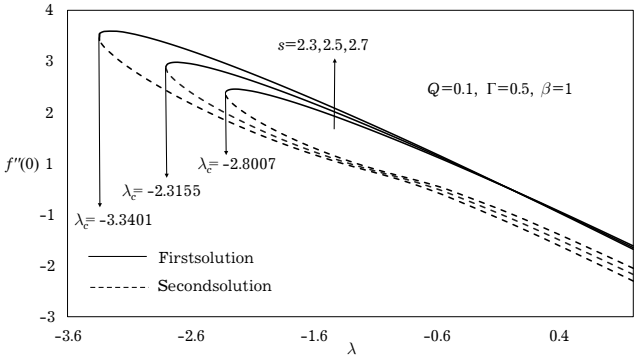

Fig. 2. Variations of $f''(0)$ with λ for different values of s when $\Gamma = 0.5$, $Q = 0.1$, $\beta = 1$.

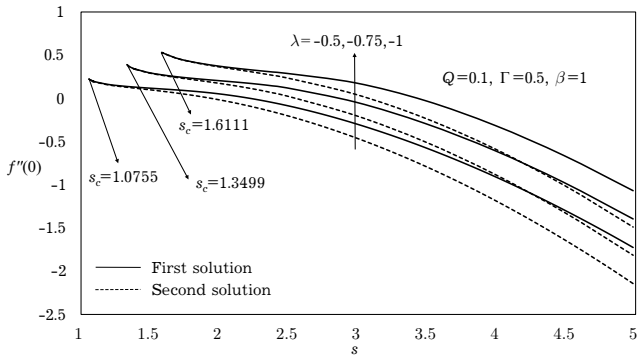

Fig. 3. Variations of $f''(0)$ with s for different values of λ when $\Gamma = 0.5$, $Q = 0.1$, $\beta = 1$.

Fig. 3 illustrates the variation of $f''(0)$ with suction s for some values of shrinking parameter λ when $\Gamma = 0.5$, $Q = 0.1$, $\beta = 1$. The figure demonstrate the increasing trend of skin coefficient for first and second solution which can be seen in Table 3. It is also can be noticed that both first and second solutions only exist on interval $s_c < s$ where s_c is the critical value of suction. Unique solution only can be observed on $s = s_c$ and no solution exists when $s < s_c$. Moreover, the increasing of stretching or shrinking parameter $|\lambda|$ cause the critical value of suction which needed to keep the boundary layer together is also increases. As the suction increases, the value of shear wall stress is decreasing.

The influence of slip boundary condition parameter, Γ on the skin friction coefficient is shown in Fig. 4. The values are noticed to decrease with the increasing of Γ in the initial segment of dual solutions for $f''(0)$. However as λ increasing, both solutions express declining trend. As shown in the Table 4, the values of $|\lambda_c|$ increases as the value of slip parameter Γ increases. The wall shear stress decreases when the slip parameter increases, thus the weakening of fluid adhesion strength occur because of the vorticity generated by shrinking sheet is reduced.

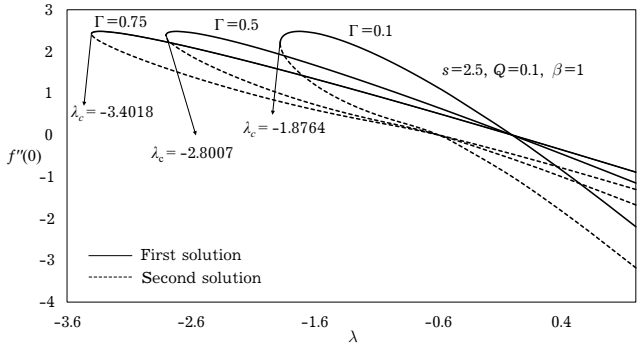

Fig. 4. Variations of $f''(0)$ with λ for different values of Γ when $s = 2.5$, $Q = 0.1$, $\beta = 1$.

Figs. 5–9 demonstrate the velocity profiles for some values of s, Q, β, λ and Γ. All figures follow the pattern of the profile asymptotically. It can be noticed that the boundary layer thickness for the second solution is bigger than the first solution. The values of $f'(\eta)$ are all negatives throughout the profiles.

The effects of suction s on velocity profiles is shown in Fig. 5. As the value of suction increases, there is an increment in the value of $f'(\eta)$ in the first solution while there is reduction for second solution. The boundary layer thickness for first solution is noticeable to be smaller as s increases, oppositely for second solution. Suction able to reduce the thickness of boundary layer which in the end force the flow of fluid to move slower and closer to boundary, thus elevate the velocity gradient at the sheet surface.

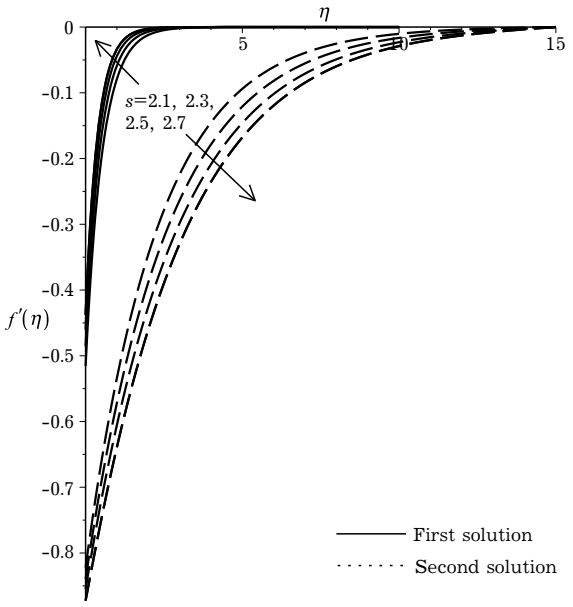

Fig. 5. Velocity profiles $f'(\eta)$ for several values of s when $\Gamma = 0.5$, $Q = 0.1$, $\beta = 1$, $\lambda = -1$.

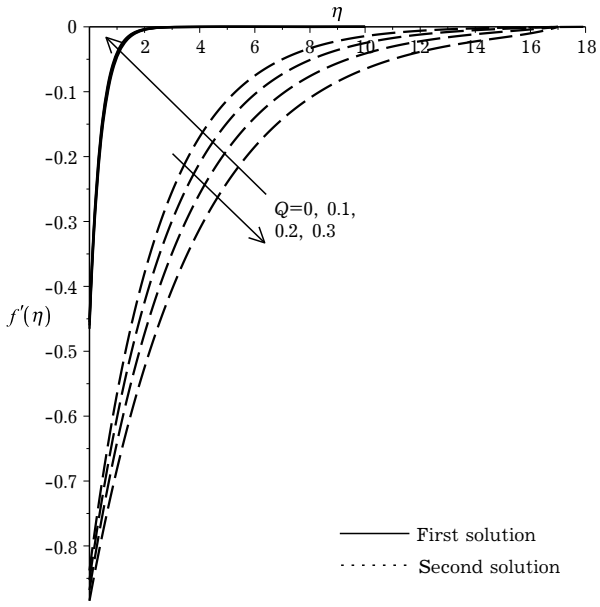

Fig. 6. Velocity profiles $f'(\eta)$ for several values of Q when $s = 2.5$ $\Gamma = 0.5$, $\beta = 1$, $\lambda = -1$.

Fig. 6 shows the velocity profiles of several values of Q which is Chandrasekhar number on $f'(\eta)$. The increment in Q causes the $f'(\eta)$ in first solution increase while contrarily for second solution. The boundary layer thickness seems to be smaller when values of Q increases. However, it works differently for second solution whereas, the boundary layer thickness becomes larger for second solution. The velocity profiles is improved and reduced the thickness of boundary layer because of the existence of Lorentz force.

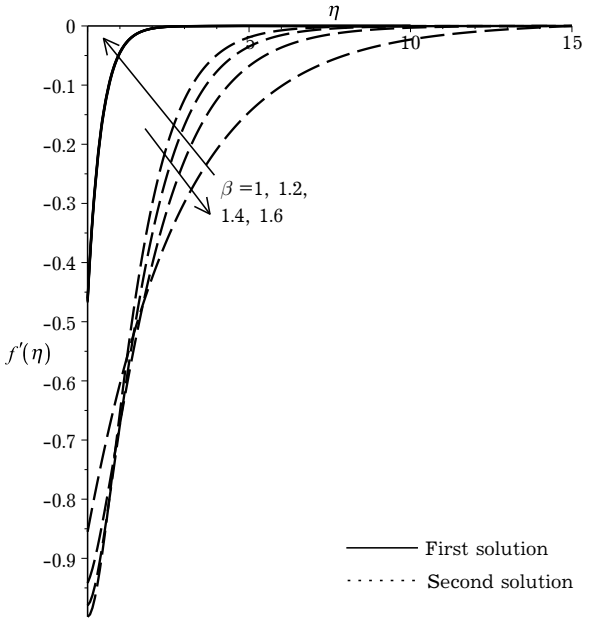

Fig. 7. Velocity profiles $f'(\eta)$ for several values of β when $\Gamma = 0.5$, $Q = 0.1$, $s = 2.5$, $\lambda = -1$.

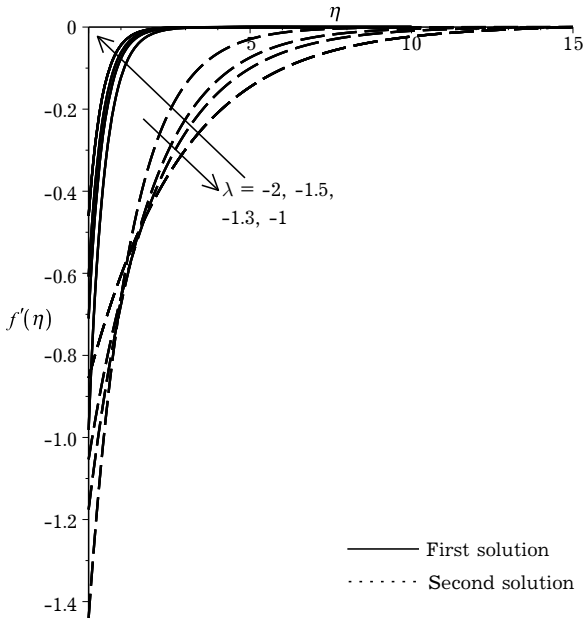

Fig. 8. Velocity profiles $f'(\eta)$ for several values of λ when $s = 2.5$, $\Gamma = 0.5$, $Q = 0.1$, $\beta = 1$.

The velocity profiles of several values of nonlinear parameter, β is shown in Fig. 7. It is also known as Casson parameter. As the values of β increases, $f'(\eta)$ in first solution increases and decrease in second solution. The thickness of boundary layer decrease when the values of β increases. The yield stress is smaller compared to the viscosity and deformation when the values of β increases.

Fig. 8 displays the influence of shrinking/stretching parameter λ on the velocity profile $f'(\eta)$. In the shrinking case where $\lambda < 0$, the increasing of $|\lambda|$ caused the value of $f'(\eta)$ to reduce in first solution and increase in second solution. Thus, the thickness of boundary layer becomes larger in the first solution when $|\lambda|$ increases. Moreover, the increasing value of $|\lambda|$ allows more fluid flow towards the opposite direction in the sheet. Therefore, the velocity moves away and the thickness of boundary layer improved.

Next, Fig. 9 illustrates the velocity profiles $f'(\eta)$ for different values of slip parameter Γ for the shrinking sheet ($\lambda < 0$) case. From the figure shown, it can be seen that for the values of velocity profile $f'(\eta)$ increases with the increment in the value of slip parameter Γ. On another hand, the values of velocity profiles $f'(\eta)$ for second solution increases in certain initial range of η and decrease after that range. Basically, this means the increment value of slip permits more fluid flow through the surface, thus decreasing the thickness of boundary layer and enhancing the velocity gradient of the first solution.

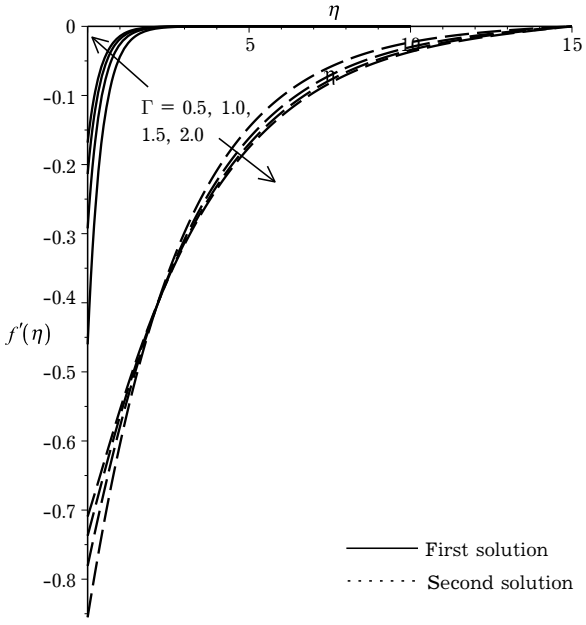

Fig. 9. Velocity profiles $f'(\eta)$ for several values of Γ when $s = 2.5$, $Q = 0.1$, $\beta = 1$, $\lambda = -1$.

4. Conclusion

In this research, the effect of MHD flow over stretching or shrinking sheet with suction and Navier slip is theoretically and numerically studied. The problem was solved by using the Shooting Method in Maple software. The effects of the governing parameters toward the skin friction coefficient and velocity profile are illustrated in graphs and discussed in detail. Following those results, we can conclude that:

1) The increment of λ and s increases the values of skin coefficient friction.
2) The increment of Γ decreases the values of skin coefficient friction.
3) The velocity profiles escalate with the increasing s, λ, β, Γ and Q.

Acknowledgement

The authors gratefully acknowledge the financial support received in the form of a research grant from University Putra Malaysa, Malaysia (Vot no: GP-UPM/2018/9619000). The authors would also like to express their thanks to the very competent reviewers for the very good comments and suggestions.

[1] Crane L. J. Flow past a stretching plate. Zeitschrift für angewandte Mathematik und Physik ZAMP. **21** (4), 645–647 (1970).

[2] Gupta P. S., Gupta A. S. Heat and mass transfer on a stretching sheet with suction or blowing. The Canadian Journal of Chemical Engineering. **55** (6), 744–746 (1977).

[3] Rajagopal K. R., Na T. Y., Gupta A. S. Flow of a viscoelastic fluid over a stretching sheet. Rheologica Acta. **23** (2), 213–215 (1984).

[4] Vajravelu K. Viscous flow over a nonlinearly stretching sheet. Applied Mathematics and Computation. **124** (3), 281–288 (2001).

[5] Partha M. K., Murthy P. V. S. N., Rajasekhar G. P. Effect of viscous dissipation on the mixed convection heat transfer from an exponentially stretching surface. Heat and Mass Transfer. **41** (4), 360–366 (2005).

[6] Sajid M., Hayat T. Influence of thermal radiation on the boundary layer flow due to an exponentially stretching sheet. International Communications in Heat and Mass Transfer. **35** (3), 347–356 (2008).

[7] Bidin B., Nazar R. Numerical solution of the boundary layer flow over an exponentially stretching sheet with thermal radiation. European journal of scientific research. **33** (4), 710–717 (2009).

[8] Khan W. A., Pop I. Boundary-layer flow of a nanofluid past a stretching sheet. International Journal of Heat and Mass Transfer. **53** (11–12), 2477–2483 (2010).

[9] Rana P., Bhargava R. Flow and heat transfer of a nanofluid over a nonlinearly stretching sheet: a numerical study. Communications in Nonlinear Science and Numerical Simulation. **17** (1), 212–226 (2012).

[10] Hsiao K. L. Stagnation electrical MHD nanofluid mixed convection with slip boundary on a stretching sheet. Applied Thermal Engineering. **98**, 850–861 (2016).

[11] Daniel Y. S., Aziz Z. A., Ismail Z., Bahar A., Salah F. Slip role for unsteady MHD mixed convection of nanofluid over stretching sheet with thermal radiation and electric field. Indian Journal of Physics. **94** (2), 195–207 (2020).

[12] Wang C. Y. Liquid film on an unsteady stretching surface. Quarterly of Applied Mathematics. **48** (4), 601–610 (1990).

[13] Miklavčič M., Wang C. Viscous flow due to a shrinking sheet. Quarterly of Applied Mathematics. **64** (2), 283–290 (2006).

[14] Fang T., Zhang J. Closed-form exact solutions of MHD viscous flow over a shrinking sheet. Communications in Nonlinear Science and Numerical Simulation. **14** (7), 2853–2857 (2009).

[15] Fang T., Zhang J., Yao S. Slip MHD viscous flow over a stretching sheet – an exact solution. Communications in Nonlinear Science and Numerical Simulation. **14** (11), 3731–3737 (2009).

[16] Fang T., Yao S., Zhang J., Aziz A. Viscous flow over a shrinking sheet with a second order slip flow model. Communications in Nonlinear Science and Numerical Simulation. **15** (7), 1831–1842 (2010).

[17] Sarpkaya T. Flow of non-Newtonian fluids in a magnetic field. AIChE Journal. **7** (2), 324–328 (1961).

[18] Pavlov K. Magnetohydrodynamic flow of an incompressible viscous fluid caused by deformation of a plane surface. Magnitnaya Gidrodinamika. **4** (1), 146–147 (1974).

[19] Mahabaleshwar U. S., Nagaraju K. R., Sheremet M. A., Vinay Kumar P. N., Lorenzini G. Effect of Mass Transfer and MHD Induced Navier's Slip Flow Due to a non Linear Stretching Sheet. Journal of Engineering Thermophysics. **28** (4), 578–590 (2019).

[20] Abdal S., Ali B., Younas S., Ali L., Mariam A. Thermo-Diffusion and Multislip Effects on MHD Mixed Convection Unsteady Flow of Micropolar Nanofluid over a Shrinking/Stretching Sheet with Radiation in the Presence of Heat Source. Symmetry. **12** (1), 49 (2020).

[21] Navier C. Mémoire sur les lois du mouvement des fluides. Mémoires de l'Académie Royale des Sciences de l'Institut de France. **6** (1823), 389–440 (1823).

[22] Masmoudi N., Saint-Raymond L. From the Boltzmann equation to the Stokes–Fourier system in a bounded domain. Communications on Pure and Applied Mathematics: A Journal Issued by the Courant Institute of Mathematical Sciences. **56** (9), 1263–1293 (2003).

[23] Iftimie D., Sueur F. Viscous boundary layers for the Navier–Stokes equations with the Navier slip conditions. Archive for Rational Mechanics and Analysis. **199** (1), 145–175 (2011).

[24] Das S., Jana R. N. Entropy generation due to MHD flow in a porous channel with Navier slip. Ain Shams Engineering Journal. **5** (2), 575–584 (2014).

[25] Matin M. H., Khan W. A. Electrokinetic effects on pressure driven flow of viscoelastic fluids in nanofluidic channels with Navier slip condition. Journal of Molecular Liquids. **215**, 472–480 (2016).

[26] Tlili I., Hamadneh N. N., Khan W. A. Thermodynamic analysis of MHD heat and mass transfer of nanofluids past a static wedge with Navier slip and convective boundary conditions. Arabian Journal for Science and Engineering. **44** (2), 1255–1267 (2019).

Магнітогідродинамічний індукований потік ковзання Нав'є та вплив всмоктування внаслідок нелінійного розтягування/стиснення шару

Аліас Н. С.[1], Хафідзуддін М. Е. Н.[2]

[1]*Кафедра математики,*
Університет Путра Малайзія,
43400 UPM Серданг, Селангор, Малайзія
[2]*Центр фундаментальних досліджень сільськогосподарської науки,*
Університет Путра Малайзія,
43400 UPM Серданг, Селангор, Малайзія

У цьому дослідженні розглянуто проблему магнітогідродинамічного (МГД) індукованого потоку, враховуючи всмоктування та ковзання Нав'є, на шарі, який може нелінійно розтягуватися або стискатися. Перетворення подібності використано для перетворення головних нелінійних диференціальних рівнянь у частинних похідних до системи нелінійних звичайних рівнянь. Після цього, перетворені звичайні диференціальні рівняння розв'язуються за допомогою методу стрільби в Maple Software. Подвійні розв'язки отримані для певних керуючих параметрів. Отримані результати показують, що всмоктування покращує поверхневе тертя, тоді як параметр ковзання зменшує напруження зсуву стінки. Крім того, виявлено, що область подвійного розв'язку у випадку шару, який розтягується, є меншою у порівнянні зі шаром, який стискається.

Ключові слова: *МГД, ковзання Нав'є, розтягування/стиснення шару, нелінійний, подвійний розв'язок.*